Identification of Residues in the Aromatic Substrate Binding Site of Horseradish Peroxidase by ^{1}H NMR Studies on Isozymes†

Jeffrey S. de Ropp,‡ Zhigang Chen,§ and Gerd N. La Mar*,§

Department of Chemistry and NMR Facility, University of California, Davis, California 95616

Received June 16, 1995⊗

ABSTRACT: The cyanide-inhibited complexes of two horseradish peroxidase acidic isozymes, A1 (HRP^{A1}, unsequenced) and A2 (HRP^{A2}, sequenced), have been examined by solution two-dimensional ^{1}H NMR methods, and the active site molecular and electronic structure compared to that of the well-characterized isozyme C (HRP^{C}) (Chen, Z., de Ropp, J. S., Hernández, G., & La Mar, G. N. (1994) *J. Am. Chem. Soc. 116,* 8772−8783), as well as to that of cytochrome *c* peroxidase. The identity and alignment of catalytically relevant residues near the active site for HRP^{A1}-CN and HRP^{A2}-CN are determined, and key residue replacements implicated in the differential catalytic properties of the acidic *vs* C isozymes are identified. Heme and axial His contact shift patterns, as well as dipolar contacts of residues with the heme and with each other, confirm a highly conserved structure among the three isozymes, including for the distal pocket residues involved in the activation of the enzyme. The remarkable dynamic stability of the heme pocket, as reflected in NH exchange with solvent, is also conserved for the three isozymes. An additional heme contact, Ile 148, is identified in HRP^{C}-CN. Four residues in contact with the heme in HRP^{C}-CN are replaced in HRP^{A2}-CN, two of which are likely functionally neutral, Gly 169 → Ala and Ile 148 → Leu. However, two substitutions in the acidic isozymes in the aromatic substrate binding pocket on the heme edge, Ile 244 → Leu and Phe 179 or 221 → aliphatic residue, could well account for the dramatic decrease ($\sim 10^3$) in aromatic substrate binding in the A1 and A2 isozymes *vs* the C isozyme of HRP. The identification of heme pocket substitutions provides important constraints on molecular homology models of HRP. The present NMR approach is expected to have broad applications for determination of active site structure both for genetically engineered moderately large (34−48 kDa) point mutants of heme peroxidases and for heme oxygenases.

Heme peroxidases are enzymes which carry out one-electron oxidation on a wide variety of substrates at the expense of peroxide (Dunford, 1991; Welinder, 1992). The mechanism of activation of heme peroxidases to two oxidizing equivalents above the ferric resting state appears to take a common pathway originally elucidated on the basis of the crystal structure of cytochrome *c* peroxicase, C*c*P,[1] and proposed to be generally operative in heme peroxidases on the basis of sequence homology for certain active site residues (Poulos & Kraut, 1980; Ortiz de Montellano, 1992). The conserved residues are a proximal Asp that hydrogen bonds to the conserved ligated His and stabilizes high oxidation states for the heme iron and both a distal cationic side chain (Arg) and a general base (His) that facilitate heterolytic Fe^{III}−OOR bond cleavage. Recent crystal studies on two fungal peroxidases, lignin peroxidase (LiP) (Edwards *et al.*, 1993) and manganese peroxidase (MnP) (Sundaramoorthy *et al.*, 1994), and isozyme E5 of plant horseradish peroxidase (HRP) (Morita *et al.*, 1993) have confirmed largely conserved residues for activation of the enzymes. However, while the strong sequence homology for active site residues translates into a highly conserved molecular structure of key residues near the peroxide binding site, there is little sequence homology observed (Welinder & Gajhede, 1993) among diverse bacterial, fungal, and plant peroxidases in the regions of the protein involved in substrate binding (see below). Competitive binding (Schonbaum, 1973) as well as spectroscopic studies (Sakurada *et al.*, 1986) have revealed that the peroxide (heme iron) and substrate binding sites are not the same. Elegant suicide inhibitor studies (Ator & Ortiz de Montellano, 1987; Ortiz de Montellano, 1987) with hydrazines on a variety of peroxidases lead to δ−meso substitution of the heme, indicating a substrate pocket at the heme periphery near the junction of pyrrole A and D (see Figure 1).

HRP, a prototypical plant peroxidase, can be isolated as numerous natural isozymes with similar activation rates but high differential affinity toward substrates (Shannon *et al.*, 1966; Kay *et al.*, 1967; Reimann & Schonbaum, 1978). Isozyme C (HRP^{C}) is the most studied heme peroxidase [including its successful expression (Smith *et al.*, 1990)] but has to date failed to yield crystals suitable for high-resolution X-ray studies. The HRP isozymes, as a group, differ from

† This research was supported by a grant from the National Institutes of Health (GM 26226). The NMR spectrometer was purchased in part with funds provided by the National Institutes of Health (RR 04795) and National Science Foundation (BBS 88-04739).

* Address correspondence to Prof. Gerd N. La Mar, Department of Chemistry, University of California, Davis, CA 95616. Telephone: (916) 752-0958. Fax: (916) 752-8995. E-mail: lamar@indigo.ucdavis.edu.

‡ NMR Facility.

§ Department of Chemistry.

⊗ Abstract published in *Advance ACS Abstracts,* September 15, 1995.

[1] Abbreviations: NMR, nuclear magnetic resonance; ppm, parts per million; DSS, 2,2-dimethyl-2-silapentane-5-sulfonate; HRP, horseradish peroxidase; C*c*P, cytochrome *c* peroxidase; WEFT, water-eliminated Fourier transform; LiP, lignin peroxidase; MnP, manganese peroxidase; BHA, benzhydroxamic acid; NOESY, two-dimensional nuclear Overhauser spectroscopy; TOCSY, two-dimensional total correlation spectroscopy; pI, isoelectric point.

0006-2960/95/0434-13477$09.00/0

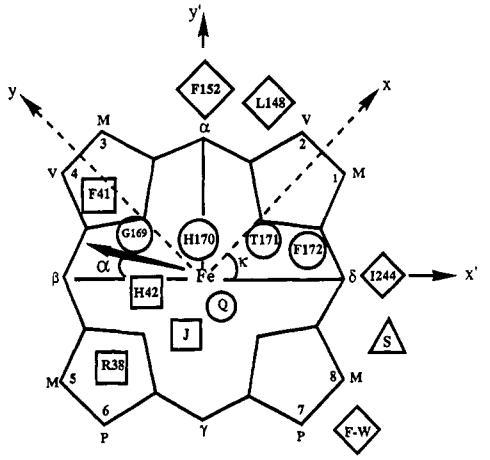

FIGURE 1: Schematic representation of the active site of HRP, with heme viewed face-on. Proximal, peripheral, and distal amino acids are represented with circles, diamonds, and squares, respectively. The amino acid-numbering scheme follows that of the HRP^{C} isozyme. The postulated substrate (triangle) binding site is near the pyrrole A/D junction. The figure also illustrates the definition of the magnetic axes of the heme, with the bold arrow indicating the direction of tilt of the major magnetic axis (see text) (in HRP^{A2}, L243 replaces I244 and A168 replaces G169; in addition, the alignment of residues in the proximal environment is offset one residue number such that H170-T171-F172 in HRP^{C} becomes H169-T170-F171 in HRP^{A2}, see Figure 2).

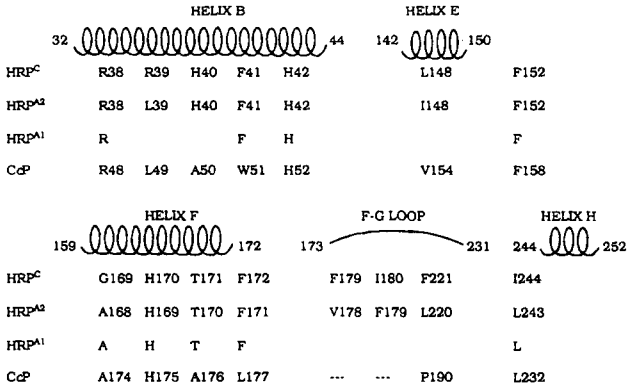

FIGURE 2: Alignment of key heme pocket amino acid residues of HRP^{C}, HRP^{A2}, and CcP (Welinder, 1992; Welinder & Gajhede, 1993) and positions of these residues relative to helices and loops as determined in the CcP crystal structure. The placement of HRP^{A1} residues, where possible, follows from data presented here. Dashes indicate deletions in the CcP sequence. Helices and loops are numbered according to HRP^{C}.

the structurally characterized peroxidases in numerous sequential insertions that occur near the proposed substrate binding pocket. In the absence of crystals, considerable emphasis has been placed on solution ^{1}H NMR structure determination, most successfully in the low-spin, cyanide-inhibited complex (de Ropp *et al.*, 1984, 1991; Gonzalez-Vergara *et al.*, 1985). In fact, a combination of one-dimensional (1D) and two-dimensional (2D) NMR methods applied to HRP^{C}-CN has not only uniquely identified the key distal site residues involved in peroxide activation but also allowed semiquantitative comparison with CcP and LiP of the disposition of these residues relative to each other and the heme (Chen *et al.*, 1994). A combination of analysis of relaxation of substrate protons by the iron (Sakurada *et al.*, 1986) and steady state NOEs from the heme 8-CH_3 to substrate and an Ile residue (La Mar *et al.*, 1992), as well as dipolar connections (NOESY) between substrate and one (labeled Phe-W here) of two interacting Phes (Veitch & Williams, 1990), has thus identified the type, but not the sequence location, of key residues near the heme edge where the substrate binds.

More recently, homology-modeling studies have produced molecular models for HRP^{C}, whose construction demanded assumptions on the sequence homology between HRP^{C} and the structurally characterized CcP or LiP (Smith *et al.*, 1995; Banci *et al.*, 1994). The models suffer from a degree of uncertainty enhanced by the fact that there is a long insertion of residues (179−213 between the F and G helices) in HRP^{C} for which there are no homologues in CcP (the situation is similar for HRP *vs* LiP), and there is a 19-amino acid insertion in CcP between residues 241 and 242 of HRP^{C}, near the beginning of helix H. The less well-established F−G and G−H loops of HRP both contain residues implicated by molecular modeling (or NMR) as prominent features of the active site. The models agreed in predicting that Ile 180 in HRP^{C}, rather than the Ile 244 suggested by comparison to CcP (Chen *et al.*, 1994), is in contact with pyrrole D but could not provide definitive information on the origin of Phe-W. The simultaneous development of the 2D NMR methods for paramagnetic enzymes and the computational modeling necessary to study such large enzymes suggests that homology and NMR studies could, in concert, provide a more accurate description of the molecular structure of HRP than either approach alone.

Since heme peroxidases are too large to effectively embark on sequence specific assignment of residues based solely on homonuclear NMR technology (La Mar & de Ropp, 1993: Chen *et al.*, 1994), one strategy is to construct selected point mutants on the basis of identified contacts of interest (*i.e.*, Ile and Phe). In order to limit the targets for point mutagenesis, we have elected initially to investigate natural isozymes of HRP that show variability in substrate binding (Reimann & Schonbaum, 1978) and for which available sequence data indicate substitution for some of the Ile and Phe. Relevant portions of the amino acid sequences of isozymes HRP^{C} and A2 (HRP^{A2}) are shown in Figure 2, along with those of CcP for comparison. Earlier low-resolution unassigned ^{1}H NMR of the cyanide complex had directly shown that the two HRP isozymes are similar (Gonzalez-Vergara *et al.*, 1985), particularly with respect to the hyperfine-shifted peaks, and suggests very similar molecular and electronic structures. In this report, we pursue detailed ^{1}H NMR studies of active site residues of the sequenced HRP^{A2}-CN and the unsequenced HRP^{A1}-CN complexes (also referred to as the acidic isozymes due to their pI values) and compare molecular and electronic structure with similar data presented recently (Chen *et al.*, 1994) from HRP^{C}-CN. Particular attention will be placed on identification of the type of residue near the substrate binding site. Previous binding studies (Reimann & Schonbaum, 1978) of the substrate benzhydroxamic acid (BHA) have shown that its binding to the acidic isozymes is significantly reduced ($K_d \sim 10^{-3}$ M) when compared to that of HRP^{C} ($K_d \sim 10^{-6}$ M), implying different structures for the substrate binding site for the acidic isozymes compared to that in isozyme C. We show that the available NMR data indicate a highly conserved molecular/electronic structure among the A1, A2, and C isozymes, but with two significant substitutions in the substrate binding site that may govern the different affinities toward substrates.

MATERIALS AND METHODS

Proteins. Purified HRP acidic isozymes type VII and type VIII were purchased from Sigma as lyophilized salt-free powders. Sigma acidic isozyme type VII is HRP^{A2}, in the nomenclature of Welinder (Welinder, 1992).[2] Sigma type VIII is isozyme A1 in Welinder's nomenclature as denoted here and labeled HRP^{A1}. Proteins were dissolved in either 99.96% ^2H_2O or 90% H_2O/10% ^2H_2O to form solutions of ~1 mM in HRP^{A2} or ~2 mM in HRP^{A1} in 5 mm tubes for NMR study. Cyanide ligation was generated by addition of 2−3 equiv of KCN to the protein solution. Solution pH (not corrected for isotope effect) was adjusted with small amounts of dilute ^2HCl or NaO^2H.

^1H NMR Spectra. 1D and 2D (NOESY, WEFT-NOESY, and CLEAN-TOCSY) NMR spectra were obtained on a GE NMR Ω 500 MHz spectrometer as described in detail previously (Chen *et al.*, 1994) for the cyano complex of HRP^C. NOESY data utilized a mixing time of 20 ms; CLEAN-TOCSY mixing times of 9−25 ms were used as described previously. Data processing was identical to the methods previously described; specific details of data collection and processing parameters are included in the figure captions as necessary. All chemical shifts were referenced to the solvent peak which had previously been calibrated against internal 2,2-dimethyl-2-silapentane-5-sulfonate, DSS. 1D saturation transfer experiments were conducted on samples in 90% ^1H_2O. Data were collected using a 1331-pulse sequence (Hore, 1983), interleaving data sets where the solvent was irradiated with data sets having the irradiation off-resonance. The saturation fraction is the residual peak height of exchangeable resonances in the difference spectra of the two data sets (Campbell *et al.*, 1977).

RESULTS

The resolved portions of the 500 MHz ^1H NMR spectra of HRP^C-CN, HRP^{A2}-CN, and HRP^{A1}-CN in ^2H_2O at 45 °C are shown in parts A, B, and D, respectively, Figure 3; not shown for each complex is a broad single proton peak in the −25 to −32 ppm window (but whose shift is listed in Table 1). The positions of resolved hyperfine-shifted labile single proton peaks present in ^1H_2O are shown by arrows and dashed lines. The WEFT spectrum of HRP^{A2}-CN is illustrated in Figure 3C, which reveals moderately to strongly relaxed proton signals in a manner previously described in detail for HRP^C-CN (Chen *et al.*, 1994). The procedures for assigning the paramagnetically influenced active site resonances in a low-spin ferric hemoprotein have been described in detail previously and applied to obtain assignments for HRP^C-CN (Chen *et al.*, 1994). This same strategy is applied (and found successful) for the present acidic isozymes. Relevant 1D and 2D NMR data will be shown for HRP^{A2}-CN as needed to confirm key aspects of structural conservation or substitution with respect to HRP^C-CN. Similar 2D NMR data for HRP^{A1}-CN are given in the supporting information.

[2] We follow the nomenclature of Welinder for naming the acidic isozymes. This convention differs from the original designation by Shannon (Shannon *et al.*, 1966). The designation of A2 is the same in both conventions, but Shannon's A3 isozyme is now labeled A1 (K. G. Welinder, private communication) and is referred to as such herein. Thus, from the earlier report on acidic isozymes (Gonzalez-Vergara *et al.*, 1985) which used the Shannon formalism, we infer that the "A3" isozyme studied therein is what we designate as "A1" here. The highly similar one-dimensional NMR spectra in both studies corroborate this.

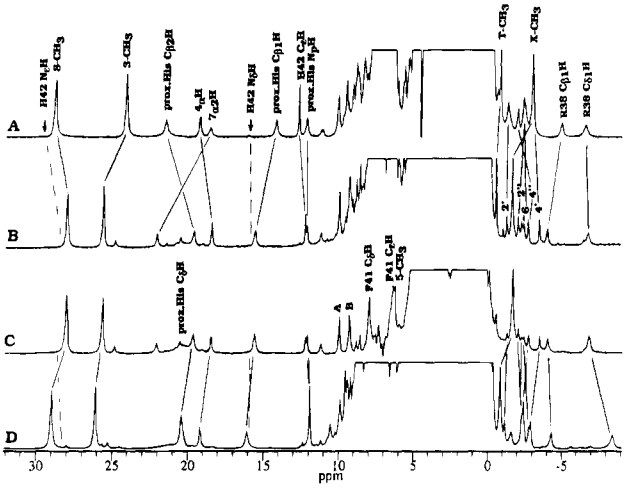

FIGURE 3: ^1H NMR (500 MHz) spectra of cyanide-ligated HRP isozymes in ^2H_2O, pH 7.0, at 45 °C: (A) HRP^C-CN (B) HRP^{A2}-CN, (C) WEFT spectrum of HRP^{A2}-CN, and (D) HRP^{A1}-CN. Spectra in A, B, and D collected at a repetition rate of 2 s^{-1}. WEFT spectrum collected with 5 s^{-1} repetition rate and a relaxation delay of 100 ms. Peak labels are (A) composite of H42 $C_\delta H$ and A169 $N_P H$ and (B) composite of H42 $N_P H$ and H169 $C_\alpha H$: 2′, $2\beta_{cis}$; 2″, $2\beta_{trans}$; 4′, $4\beta_{cis}$; 4″, $4\beta_{trans}$; and 6, $6\beta H_2$. Arrows show location of resolved exchangeable peaks detected in ^1H_2O. Solid lines connect similarly assigned peaks in the three isozymes with dashed lines reserved for the resolved exchangeable peaks. Remaining assigned peak shifts are presented in Table 1.

Coordinated Ligands. The heme resonances are assigned in the well-established manner (Satterlee & Erman, 1991; de Ropp *et al.*, 1991; La Mar & de Ropp, 1993) for a low-spin ferric heme by detection of two three-spin (heme vinyls) and two four- (not always complete) spin (heme propionates) systems with significant hyperfine shifts that exhibit NOESY cross-peaks to heme methyls; these uniquely identify the pyrrole substituents 1−8. All assigned heme resonance shifts for HRP^{A2}-CN and HRP^{A1}-CN, as well as the earlier HRP^C-CN assignments, are listed in the supporting information. The four meso-H are located by the expected NOESY cross-peaks to the two adjacent pyrrole substituents and their characteristic hyperfine shifts which extrapolate to the 10−13 ppm window in a Curie plot as described in detail for HRP^C-CN (de Ropp *et al.*, 1991). The heme side chains in HRP^{A2}-CN, HRP^{A1}-CN, and HRP^C-CN exhibit very similar hyperfine shifts and similar orientations (*i.e. trans* and *cis* for 2-vinyl and 4-vinyl, respectively, as reflected by common NOESY cross-peaks of the vinyl H_βs to the heme 3-CH_3). The only systematic difference observed among the complexes is that the spread of the $7H_\alpha$ resonances (with conserved mean shift) is larger in A2 and A1 than in C isozyme.

The axial His (residue 170 in HRP^C; 169 in HRP^{A2}) is readily recognized in all isozymes by the TOCSY-detected four-spin system (not shown) involving the $NHC_\alpha HC_\beta H_2$ fragment, all of whose signals are resolved in the normal and/or WEFT traces (Figure 3). The very broad (~300 Hz) single proton peaks that arise from the ring $C_\delta H$ near 22 ppm and $C_\epsilon H$ in the extreme upfield spectral window (not shown) are most readily detected in a WEFT trace as shown for HRP^{A2}-CN in Figure 3C. The chemical shifts for the axial His peaks are similar in the three isozymes and are listed in Table 1. The smaller spread of the $C_\beta H$ shifts in HRP^{A2}-CN (or HRP^{A1}-CN) relative to those in HRP^C-CN likely reflects a small rotation about the $C_\alpha - C_\beta$ bond. The variation in the ring CH shifts likely reflect small changes

Table 1: Chemical Shifts for Active Site Amino Acid Residues in Cyanide-Inhibited Complexes of Horseradish Peroxidase Isozymes C, A2, and A1 at 45 °C, pH 7.0, and 500 MHz[a]

	proton	HRP^{C}-CN	HRP^{A2}-CN	HRP^{A1}-CN
		Proximal Residues[b]		
Gly 169/Ala 168	N_PH	10.12	9.94	9.33
	$C_\alpha H$	5.73	5.24	5.05
	$C_\alpha H'$/ $C_\beta H_3$	4.99 ($C_\alpha H'$)	3.17 ($C_\beta H_3$)	3.07 ($C_\beta H_3$)
His 170/His 169	N_PH	12.16	12.07	11.80
	$C_\alpha H$	9.49	9.20	9.45
	$C_{\beta 2}H$	21.44	19.69	20.43
	$C_{\beta 1}H$	14.18	15.61	16.06
	$C_\delta H$	21.7	20.3	21.2
	$C_\epsilon H$	−27.4	−25.3	−27.9
Thr 171/Thr 170	N_PH	9.05	8.78	8.76
	$C_\alpha H$	*c*	5.18	5.19
Phe 172/Phe 171	N_PH	9.49	9.29	9.50
	$C_\alpha H$	5.65	5.65	5.75
	$C_\delta Hs$	7.61	7.67	7.78
	$C_\epsilon Hs$	7.16	7.29	7.19
	$C_\zeta H$	6.53	6.65	6.65
residue Q	Q-1	8.87	8.54	8.49
	Q-2	8.32	8.05	8.06
	Q-3	6.59	6.52	6.43
	Q-4	5.10	4.77	4.99
		Distal Residues		
Arg 38	N_PH	5.67	5.91	5.71
	$C_\alpha H$	0.59	1.46	1.46
	$C_{\beta 1}H$	−4.91	−4.10	−4.41
	$C_{\beta 2}H$	−0.59	−0.22	−0.50
	$C_{\gamma 1}H$	0.61	0.78	0.19
	$C_{\gamma 2}H$	−1.40	−0.27	−1.65
	$C_{\delta 1}H$	−6.56	−6.83	−8.60
	$C_{\delta 2}H$	1.02	0.48	−0.15
Phe 41	$C_\delta Hs$	7.62	7.93	8.50
	$C_\epsilon Hs$	6.34	6.36	7.72
	$C_\beta H$	2.65	3.09	*c*
His 42	N_PH	9.09	9.27	9.16
	$C_\alpha H$	4.76	*c*	4.85
	$C_\delta H$	10.03	9.88	9.85
	$N_\delta H$	16.08	15.9	15.85
	$C_\epsilon H$	12.70	12.14	11.86
	$N_\epsilon H$	29.78	28.5	28.2
residue J	J-1	6.41	5.64	5.85
	J-2	3.27	2.74	3.21
		Peripheral Residues		
Leu/Ile 148	$C_\gamma H$	0.67	0.09	*c*
(residue T)	$C_\delta H_3'$/ $C_\gamma H'$	0.76 ($C_\delta H_3'$)	0.15 ($C_\gamma H'$)	*c*
	$C_\delta H_3$	−0.74	−0.58	*c*
Phe 152	$C_\delta Hs$ or $C_\zeta H$	7.15	7.04	7.11
	$C_\epsilon Hs$	6.25	6.19	6.17
	$C_\zeta H$ or $C_\delta Hs$	5.44	5.48	5.46
Ile 244/Leu 243	$C_\gamma H$	0.21	1.44	1.63
(residue X)	$C_\gamma H'$/ $C_\delta H_3'$	1.17 ($C_\gamma H'$)	0.24 ($C_\delta H_3'$)	0.48 ($C_\delta H_3'$)
	$C_\delta H_3$	−2.87	−1.64	−0.90
Phe 221(?)/Leu 220	ring	7.73	0.78	0.69, 0.72
(residue W)	Hs/CH_3	(ring Hs)	(CH_3)	(CH_3(?))[d]

[a] Chemical shifts in ppm referenced to DSS in ^2H_2O (except for His 42 ring NHs in ^1H_2O). Shifts ± 0.01 ppm. [b] When two residues are listed, the first designation is for HRP^{C} and the second for HRP^{A2}. The HRP^{A1} sequence is unknown, and homologous resonance assignments are made on the basis of scalar and dipolar connectivities in analogy to HRP^{A2} and HRP^{C}. [c] Not located due to spectral overlap. [d] Tentative assignment indicated by (?).

in Fe−CN tilt (~1°) magnitude or direction of tilt (~10°) for the Fe−CN from the heme normal (see below) and do not reflect significant changes in either molecular or electronic structure (La Mar *et al.*, 1995).

Other Proximal Residues. The peptide NH of His 169 of HRP^{A2}-CN exhibits a series of NOESY cross-peaks in the peptide spectral window (Figure 4A), which are characteristic of NH:NH connectivities for adjacent residues with slowly exchanging NHs on a helix, and identify two NH−C_αH fragments adjacent to His 169. One of these residues exhibits TOCSY (Figure 5) and NOESY (Figure 4A) cross-peaks diagnostic of an Ala (rather than the Gly in HRP^{C}-CN) and hence identify Ala 168; the other is the backbone of Thr 170. The Ala 168 $C_\beta H_3$ exhibits strong NOESY cross-peaks to the 4-vinyl H_βs (Figure 6B), as expected from the crystal structure for the homologous Ala 174 in C*c*P. An additional slowly exchanging NH, whose chemical shift is too close to that of Thr 170 NH to exhibit a NOESY cross-peak to it, exhibits a strong NOESY cross-peak to a Phe side chain (Figure 4A) and identifies Phe 171. The same TOCSY/NOESY cross-peaks pattern (*i.e.* Ala 168 rather than Gly) is observed for HRP^{A1}-CN (see supporting information). Strong NOESY cross-peaks for His 169 $C_\beta H$ (Figure 4B) to two protons that are part of a four-spin system (Figure 5) arise from a residue which is essentially the same as the unidentified residue Q described in detail previously for HRP^{CN}-CN (Chen *et al.*, 1994); the chemical shifts are included in Table 1.

Distal Pocket Residues. Comparison of ^1H_2O and ^2H_2O solutions for HRP^{A2}-CN reveals two hyperfine-shifted labile protons at 28.5 and 15.9 ppm (dashed lines in Figure 3B) whose relaxation properties and NOESY cross-peaks (not

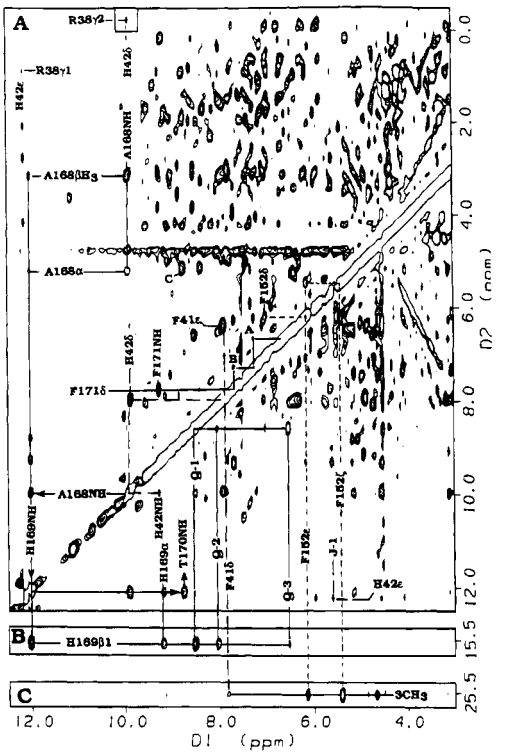

FIGURE 4: Portions of 20 ms mixing time 500 MHz NOESY spectrum of HRP^{A2}-CN in ^2H_2O, pH 7.0, at 45 °C illustrating dipolar correlations of hyperfine-influenced peaks in the downfield region. Solid lines are used to designate protons of proximal residues, long dashes protons of distal residues, and short dashes protons of peripheral residues, as defined in Table 1. A system of solid lines with arrows shows the sequential NH connectivities of the proximal residues. Assignments are described in the text. A data set of 1024 × 1024 points was processed with 30°-shifted sine-bell-squared apodization in both dimensions. Data collected with repetition rate of 5 s^{-1}. Inset at the top left of panel A was plotted at a lower contour. Peaks A, B, and C in the crowded spectral region near the center of panel A are due to F171 C_δH-F171 C_ϵH, F171 C_ϵH-F171 C_ζH, and T170 N_PH-C_αH, respectively.

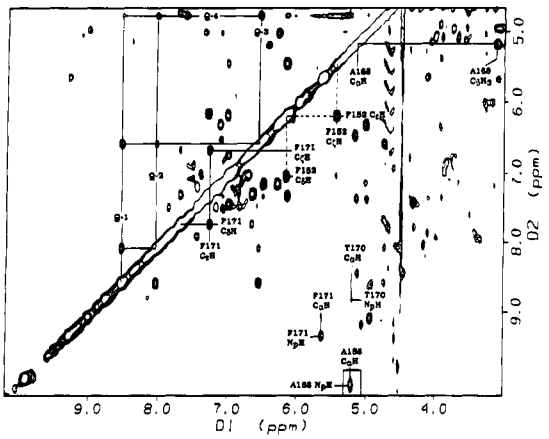

FIGURE 5: Portion of the 25 ms mixing time CLEAN-TOCSY spectrum of HRP^{A2}-CN in ^2H_2O, pH 7.0, at 45 °C showing scalar correlations of key residues in the downfield region. Solid lines designate peaks of proximal residues, and short dashes label peaks of peripheral residues. The inset at lower right was obtained at a 9 ms mixing time, which aids in detection of fast-relaxing cross-peaks (Chen *et al.*, 1994). A data set of 1024 × 1024 points, collected at a repetition rate of 5 s^{-1}, was processed with 30°-shifted sine-bell-squared apodization in both dimensions.

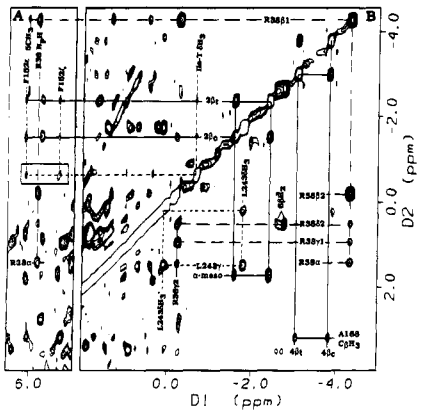

FIGURE 6: Portions of the WEFT-NOESY spectrum of HRP^{A2}-CN in ^2H_2O at a mixing time of 20 ms at 45 °C, pH 7.0, illustrating dipolar correlations of hyperfine-influenced peaks in the upfield region. Here, solid lines label proton signals of proximal residues and the heme, long dashes label protons of distal residues, and short dashes label protons of peripheral residues (as defined in Table 1). Assignments are described in the text. The inset in panel A is from a (non-WEFT) NOESY spectrum under the same conditions, allowing detection of weak cross-peaks involving the (more slowly relaxing) Phe 152 ring. Data collected and processed as in caption to Figure 4.

shown) to narrow peaks at 12.14 and 9.88 ppm uniquely identify the imidazolium side chain of His 42 as previously reported for HRP^C-CN; the strong NOE for His 42 $C_\delta H$ to an NH similarly locates the NH of His 42. Similar His 42 labile proton signals are observed for HRP^{A1}-CN (Figure 3D) and analogous His 42 assignments made (Table 1). The upfield NOESY map for HRP^{A2}-CN (Figure 6) exhibits a set of cross-peaks for an eight-spin system with three methylene groups very similar to that observed in HRP^C-CN; NOESY and TOCSY data provide sufficient connectivities (Figures 6 and 7) for uniquely identifying Arg 38 with its slowly exchanging peptide NH. NOESY cross-peaks (Figure 6) from Arg 38 C_δHs and C_βHs to 6-propionate H_βs and 5-CH_3, respectively, are also observed as reported for HRP^C-CN (Chen *et al.*, 1994). NOESY cross-peaks between Arg 38 and His 42 (Figure 4A) are also observed (His 42

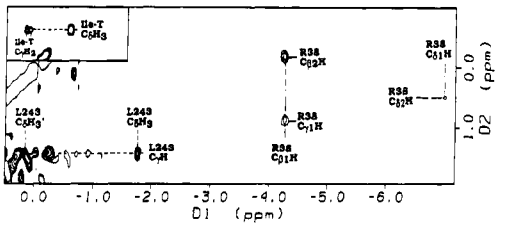

FIGURE 7: Upfield portion of the 9 ms mixing time CLEAN-TOCSY spectrum of HRP^{A2}-CN in ^2H_2O, pH 7.0, at 35 °C showing scalar connectivities of key residues in the upfield region. Long dashes label protons of distal residues and short dashes protons of peripheral residues. Inset is CLEAN-TOCSY spectrum at 45 °C with a 25 ms mixing time to improve resolution of Ile-T cross-peaks. Data collected and processed as in caption to Figure 5.

C_δH:Arg 38 $C_{\gamma 2}$H and His 42 C_ϵH:Arg $C_{\gamma 1}$H), as reported for HRP^C-CN.

The Phe 41 ring is readily identified by the NOESY cross-peak of the ring C_δH to His 42 C_δH (Figure 4A), the strong NOESY cross-peak between the Phe 41 ring protons (Figure 4A), the weak NOESY cross-peak for the Phe 41 ring to 3-CH_3 (Figure 4C), and the strong relaxation exhibited by the ring protons in the WEFT trace in Figure 3C, in a manner previously observed for HRP^C-CN. These same three distal residues (Arg 38, Phe 41, and His 42) are also identified for HRP^{A1}-CN with similar dipolar contacts (supporting information). Lastly, the His 42 C_ϵH exhibits a weak NOESY cross-peak (Figure 4A) to a proton that exhibits a spin-coupled partner and defines residue J, as reported for HRP^C-CN (Chen *et al.*, 1994). The chemical shifts for both the A2 and A1 isozymes, as well as for isozyme C, are included in Table 1.

Peripheral Heme Contacts. A Phe ring is observed in the TOCSY spectra of HRP^{A2}-CN (Figure 5) and HRP^{A1}-CN (supporting information) which is in dipolar contact with both the heme 3-CH_3 (Figure 4C) and 2-vinyl H_βs (Figure 6A), as expected for the proposed Phe 152 in HRP^C-CN (Chen *et al.*, 1994) that is conserved with respect to *Cc*P (Phe 158). We have earlier reported (Chen *et al.*, 1994) a TOCSY-detected $CHCH_3$ fragment for HRP^C-CN with a partially resolved methyl peak (residue T) in contact with the Phe 152 ring. In HRP^{A2}-CN, this residue T exhibits an upfield methyl with scalar coupling to two protons (inset of Figure 7), dictating that residue T possesses a CH_2CH_3 rather than the $CHCH_3$ fragment of HRP^C. These data argue that residue T is at a conserved position occupied by Val or Leu in HRP^C and by Ile in HRP^{A2}. The residue T, moreover, exhibits NOESY cross-peaks not only to the Phe 152 ring but also to the 2-vinyl H_βs in both HRP^{A2}-CN (Figure 6B) and HRP^C-CN (not shown). The contact of a side chain with both Phe 158 and the 2-vinyl group in the *Cc*P crystal structure is unique for Val 154. In HRP^C, this position is occupied by Leu 148, consistent with the $CHCH_3$ fragment in HRP^C-CN. In HRP^{A2}-CN, this position is occupied by Ile 148 which is consistent with the detected CH_2CH_3 fragment. Hence, we assign residue T to Leu 148 in HRP^C-CN and to Ile 148 in HRP^{A2}-CN (Figure 2). A distinction between a $CHCH_3$ and a CH_2CH_3 fragment from residue T in the Al isozyme was not possible due to spectral congestion.

An upfield-resolved methyl group, identified (de Ropp *et al.*, 1991; Chen *et al.*, 1994) as originating from an Ile-X in HRP^C-CN (based on a clearly detected CH_2CH_3 fragment by TOCSY) and proposed to arise from Ile 244 (Veitch *et al.*, 1992), is similarly observed in the two acidic isozymes

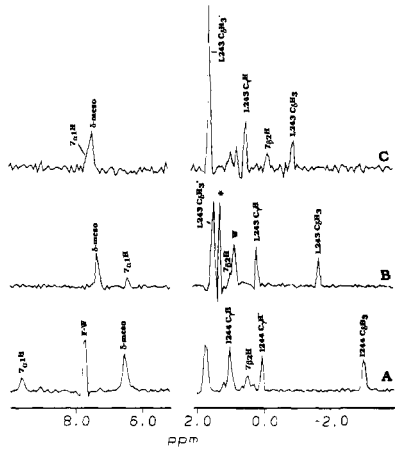

FIGURE 8: Portions of the 20 ms NOESY f_2 slices through the heme 8-CH_3 of (A) HRP^C-CN, (B) HRP^{A2}-CN, and (C) HRP^{A1}-CN at 45 °C, pH 7.0, illustrating dipolar correlations to the labeled peaks. Note the loss of F-W signal in B and C and appearance of signal W in trace B. Data collected and processed as in caption to Figure 4. * denotes an artifact.

(Figure 3B,D); in HRP^C-CN, this methyl is in dipolar contact with 8-CH_3, 1-CH_3 δ-meso-H and the proximal His $C_\epsilon H$. However, both TOCSY (Figure 7) and NOESY (Figure 6) show that this methyl in HRP^{A2}-CN results from a $CH(CH_3)_2$ rather than a CH_2CH_3 fragment and must arise from Val or Leu; a similar residue containing an isopropyl fragment (Leu/Val rather than Ile) is observed for HRP^{A1}-CN (see supporting information). The Val/Leu-X in the acidic isozymes exhibits NOESY cross-peaks to 8-CH_3 (strong, see Figure 8) and δ-meso-H (weak) but none to 1-CH_3. The Val/Leu-X methyl in HRP^{A2}-CN has a similar dipolar contact to the proximal side as in HRP^C-CN (Thanabal *et al.*, 1987), as shown by a NOE to the resolved methyl when the upfield His 169 $C_\epsilon H$ peak is saturated (not shown). We conclude that Ile-X in HRP^C is substituted by a Leu or Val-X (with largely conserved positions in the active site) in each of the acidic isozymes. Since Ile 180 of HRP^C is not conserved in HRP^{A2}, but substituted by a Phe (Figure 2), the proposed origin of Ile 180 for Ile-X (Banci *et al.*, 1994; Smith *et al.*, 1995) in HRP^C-CN can be eliminated. Ile → Val/Leu substitutions occur at only four positions in A2 relative to the C isozyme of HRP, and all but one are in relatively conserved regions (Ile 36, 80, and 103) of the structure remote from the heme, leaving Leu 243 and Ile 244 (Figure 2) as the origin for the upfield methyl signals in HRP^{A2}-CN and HRP^C-CN, respectively.

The most prominent qualitative difference in dipolar contacts for the putative substrate binding site near the pyrrole A/D junction between the A2, A1, and C isozymes is the complete loss in the acidic isozymes of a signal indicative of an aromatic side chain in contact with the heme 8-CH_3. This is shown in the 5−10 ppm spectral region in NOESY slices though the 8-CH_3 signal in parts B and C of Figure 8 for HRP^{A2}-CN and HRP^{A1}-CN, respectively, as compared to the clearly detected Phe-W signal for HRP^C-CN (Figure 8A). This Phe-W exhibits NOEs to aromatic substrates, BHA in particular (Veitch & Williams, 1990, 1991). While HRP^C-CN exhibits NOEs to peaks with chemical shifts upfield of ~1.5 ppm which all arise from either Ile 244 or 7-propionate H_β, HRP^{A2}-CN displays an additional relatively intense NOE to a peak at 0.8 ppm with minimal temperature dependence, labeled W in Figure 8B. This suggests strongly that the heme 8-CH_3 in HRP^{A2}-CN is in contact with a residue bearing a methyl group in a manner similar to the contact between 8-CH_3 and Phe-W in HRP^C-CN (Figure 8A). The weaker pair of peaks in the 1 ppm window for HRP^{A1}-CN is consistent with an interaction with the 8-CH_3 similar to that in the A2 but not the C isozyme (*i.e.* dipolar contact to an aliphatic rather than aromatic residue). Thus, we demonstrate that the Phe-W in contact with the pyrrole A/D periphery is not present in the acidic isozymes where Phe-W is likely replaced by an aliphatic residue.

The complete absence of a Phe contact to 8-CH_3 dictates that this residue is replaced by a nonaromatic side chain in the A2 and A1 isozymes. This eliminates the earlier proposal of Phe 142 (Veitch & Williams, 1990, 1991) as the origin of Phe-W, as it is conserved in HRP^{A2} (Welinder, 1992). Six Phes in HRP^C are substituted in HRP^{A2} (Phe 61, 68, 130, 143, 179, and 221), but only three are replaced by aliphatic side chains (Phe 61 → Ile 61, and Phe 179 → Val 178, and Phe 221 → Leu 220). The *Cc*P crystal structure places the homologue to Phe 61 more than 20 Å from the heme but is little help in distinguishing the Phe 179/221 possibility. Phe 179 of HRP^C is deleted in *Cc*P, and Phe 221 aligns with Pro 190, which is relatively distant (~7 Å) from the heme in *Cc*P. The similar length of Phe and Leu and the strong NOE to the 8-CH_3 of the apparent methyl group tentatively assign Phe-W to Phe 221.

Magnetic Properties of the Heme Iron. The necessarily dipolar origin of the hyperfine shifts for assigned and conserved noncoordinated heme pocket residues for which the NOESY data reflect highly conserved dispositions relative to the heme and each other (Ala 168-Phe 171, Arg 38, Phe 41, and His 42) were used as input to determine the magnetic axes for the complexes HRP^{A2}-CN and HRP^{A1}-CN, in a manner described in detail for HRP^C-CN (La Mar *et al.*, 1995). The three isozymes all produce an excellent correlation of observed and predicted dipolar shifts (see supporting information). The least-square search for the tilt (β) and direction of tilt (α) of the major axis, and the location of the rhombic axes (κ), produces values of 21° (β), −20° (α), and 60° (κ) for HRP^{A2}-CN and 22° (β), −10° (α), and 60° (κ) for HRP^{A1}-CN, which compare very well with the values reported previously for HRP^C-CN: 23° (β), −20° (α), and 70° (κ). Hence, there are minimal systematic changes in orientation of the magnetic axes (and hence Fe−CN tilt) among the three isozymes. Small shift changes for several signals such as the His 169 ring CHs and Arg 38 C_δHs could be accounted for by small changes in Fe−CN tilt (~1°) or small changes (~0.2 Å) in the position of the side chain terminus of Arg 38.

Dynamic Properties. All three isozymes exhibit strong NOESY and/or TOCSY peaks involving the peptide NHs of distal Arg 38, His 42, and the proximal residues 168−172, dictating dynamically stable proximal and distal helices to which solvent has highly limited access. The distal His 42 side chain $N_\epsilon H$, on the other hand, exhibits comparable saturation transfer with solvent in the three isozymes (data not shown), indicating that the exchange lifetime at pH 7 is comparable to T_1 ~ 20 ms, as previously determined for HRP^C-CN (Thanabal *et al.*, 1988). The very similar saturation factors (and line widths) of the N_ϵHs for His 42 for the three isozymes (not shown) indicate similar access of solvent to the heme iron vicinity.

DISCUSSION

Assignment of Residues. Our present results confirm that 1D and 2D NMR experiments, suitably tailored to detect broad relaxed lines in the presence of a large number of weakly relaxed protons, can yield definitive assignments of the active site of low-spin hemoproteins of ~45 kDa size. The homologues of nearly all residues in HRP^C-CN, which had previously been located in devising the experimental approach (Chen *et al.*, 1994), are similarly identified in HRP^{A2}-CN and HRP^{A1}-CN. The retention of backbone NHs in the proximal or F helix and the distal or B helix (Figure 2) of the active site in all isozymes long after dissolution of the proteins in ^2H_2O allows sequence specific assignments via standard backbone connectivities, as reported for HRP^C-CN. In numerous cases, it was possible not only to clearly define expected substitution in the active site based on sequence information [*i.e.* Gly 169 (HRP^C) → Ala 168 (HRP^{A2})] but also to detect substitution [Ile (HRP^C) → Leu (HRP^{A2})] for residues whose assignments were in dispute (*i.e.* Ile 180 or 244?) and for residues whose assignments had not been previously addressed [Leu 148 (HRP^C) → Ile 148 (HRP^{A2})] (Figure 2). Although sequence data on HRP^{A1} has not been reported, the present study shows evidence for close homology between the acidic isozymes (see Table 1) both in sequence alignment (Figure 2) and in dipolar contacts between residues and between residues and the heme (supporting information). The similar structures are also reflected in similar K_d values for substrate (Reimann & Schonbaum, 1978) and specific activity (Kay *et al.*, 1967) values for HRP^{A2} and HRP^{A1}.

The success in identification of the type of side chain in contact with specific portions of the heme and the demonstration of changes in the type of residue present in alternate natural genetic variants provide important constraints on the construction of viable molecular models for such large proteins. We infer that this approach will have similar success not only with the cyanide-inhibited synthetic variants of HRP but also for heme oxygenase complexes (Hernandez *et al.*, 1994).

Structural Conservation among HRP Isozymes. The proximal helix which contains the ligated His has the same orientation in the acidic isozymes relative to the heme as in HRP^C-CN or C*c*P-CN, as witnessed by the Ala 168 $C_\beta H_3$ to 4-vinyl (H_β) NOESY cross-peaks. The three distal residues observed in the acidic isozymes, Arg 38, Phe 41, and His 42, also reflect intra- and inter-residue, as well as residue−heme, NOESY cross-peak patterns and relaxation behavior essentially identical to those observed in HRP^C-CN and predicted by comparison with the C*c*P crystal structure (Finzel *et al.*, 1984). The apparent complete conservation of the activating machinery accounts for the similar formation of compound I with peroxide for all HRP isozymes and C*c*P. The present study further extends the similarity in active site structures between HRP^C and C*c*P by demonstrating that the end of the E helix, which in C*c*P contains Val 154 and Phe 158 that are in contact with both each other and the pyrrole A/B junction, is similarly positioned in HRP^C-CN with residues Phe 152 and Leu 148 and in HRP^{A2}-CN with Phe 152 and Ile 148 (Figure 2).

The strong molecular structural conservation of the heme proximal and distal environments also expresses itself in largely conserved electronic structure. The dipolar shift for the noncoordinated residues are semiquantitatively interpreted, as described in detail elsewhere for HRP^C-CN (La Mar *et al.*, 1995), by a tilt of the major magnetic axis (and Fe−CN unit) from the heme normal toward the δ−meso position that is essentially indistinguishable among the three isozymes and similar to that observed in the C*c*P-CN crystal structure (Edwards & Poulos, 1990). The small variation in shifts (such as for Arg 38 $C_\delta H$s or the axial His ring CHs) can arise from position changes from the side chain terminus of as little as 0.2 Å or could result for changes in ligand tilt of as little as 1°, which is below the uncertainty in the determination. The small change in heme hyperfine shifts (supporting information), which are primarily contact in origin, likely reflect a direct electronic influence upon the loss of an aromatic contact to pyrrole D in the acidic isozymes. The increased spread of 7H_α shift in the acidic isozymes likely indicates a bond rotation of the propionate group.

Having established that most of the heme vicinity exhibits highly conserved molecular and electronic (magnetic) structure among the HRP isozymes (and for each with C*c*P), it is possible to address small but systematic differences in the active site based on substitution of residues between isozymes C and A2. The replacement of an Ile in contact with pyrrole D and the axial His ring in HRP^C-CN with a similarly positioned Leu in the acidic isozymes establishes that Ile 244 (HRP^C) and Leu 243 (HRP^{A2} and HRP^{A1}) occupy positions similar to that of Leu 232 in C*c*P (Figure 2). This suggests that Ile 244/Leu 243 in HRP are similarly positioned at the beginning of helix H as found in C*c*P. Moreover, it demands that the 34-residue insertion (residues 179−213) in HRP relative to C*c*P occurs so as to accommodate large conserved F (proximal) and H helices. The identification of Ile 244 rather than Ile 180 as the contact to pyrrole D is in contrast to the current homology models (Banci *et al.*, 1994; Smith *et al.*, 1995). It has been noted, however, if altered sequence alignments for HRP relative to C*c*P are used, one model places Ile 244 and Phe 221 near pyrrole D (Banci *et al.*, 1994), as observed in the NMR data. It is clear that computational modeling will advantageously guide NMR assignment strategies and that the NMR results will help discriminate among alternate models in the refinement procedure.

Two unassigned residues located previously in HRP^C-CN (Chen *et al.*, 1994) that make contact with the proximal His (residue Q) and distal His 42 (residue J), respectively, are conserved in the two acidic isozymes, both in the pattern of their NOESY cross-peaks and their (likely incomplete) spin topology, with one difference noted. While the Q system in HRP^C-CN and HRP^{A2}-CN shows TOCSY correlations among all four spins at short mixing times and aliphatic variable temperature (VT) intercepts [Figure 5 and Chen *et al.* (1994)], the Q system in HRP^{A1}-CN shows a different spin topology of fewer couplings between Q protons (supporting information) along with VT intercepts closer to the aromatic region (not shown). Neither Q nor J yielded sufficient NMR data to uniquely identify the amino acid type. Since residue contacts with the proximal and distal His are not conserved between C*c*P and HRP-CN, assignments are only speculative. One homology model (Smith *et al.*, 1995) proposed Leu 250 as residue Q, which is consistent in that this Leu is conserved between isozyme C and A2. Once the sequence of isozyme A1 is known, the identity of Q and J should be clearer, as J is likely a conserved aliphatic residue in all three isozymes located near the end of the B−C loop

(which has residues in contact with the distal His $C_\epsilon H$); while Q would likely be a conserved aliphatic residue in HRP^C and HRP^{A2} but replaced in HRP^{A1} at the end of the F–G loop or the beginning of the G helix (with dipolar contacts to the proximal His $C_\beta Hs$).

Substrate Binding Site. The present study rules out Phe 142 in HRP^C as the aromatic residue in contact with both substrate and the heme edge and proposes Phe 221 (or possibly 179) as the identity of this residue, on the basis of the loss of an aromatic contact to the 8-CH_3 in HRP^{A2} and its replacement by an apparent aliphatic side chain. One molecular-modeling study had predicted Phe 68 (Banci *et al.*, 1994) as the aromatic residue in contact with 8-CH_3 and substrate; another (Smith *et al.*, 1995) has proposed Phe 221 for this residue. The present NMR results support this aspect of the latter study. The replacement of a Phe-W residue in HRP^C with an aliphatic residue in the acidic isozymes may account for severly reduced binding by the substrate BHA in HRP^{A2} and HRP^{A1} ($K_d \sim 10^{-3}$ mM) relative to HRP^C ($K_d \sim 10^{-6}$ mM) (Reimann & Schonbaum, 1978), as well as the much higher specific activity (by ~10) of the acidic isozymes (Kay *et al.*, 1967). It is noted that, while Ile 244 in HRP^C-CN is in contact with both pyrrole A (1-CH_3) and D (8-CH_3), the $C_\delta H_3$ of Leu 243 in HRP^{A2}-CN is in contact only with pyrrole D (8-CH_3). While dipolar contacts between substrate and Ile 244 in HRP^C-CN have not been detected (Thanabal *et al.*, 1987) by ^1H NMR, both Ile and substrate make strong dipolar contacts to the same heme edge (La Mar *et al.*, 1992; Chen *et al.*, 1994), near pyrroles D and A, raising the possibility that both the Phe 221 (179?) → Leu (Val) substitution and the Ile 244 → Leu 243 substitution influence substrate binding. NMR studies on point mutants of HRP aimed at separately confirming the identity of Phe-W and Ile-X, as well as assessing the separate consequences on functional properties, are planned.

SUPPORTING INFORMATION AVAILABLE

One table showing the chemical shifts for the heme as cyanide-inhibited complexes of isozymes C, A2, and A1 of horseradish peroxidase and six figures showing portions of the low-field 20 ms mixing time 500 MHz WEFT-NOESY spectrum of HRP^{A1}-CN, portions of the downfield 25 ms mixing time CLEAN-TOCSY spectrum of HRP^{A1}-CN, portions of the upfield 20 ms mixing time WEFT-NOESY spectrum of HRP^{A1}-CN, an upfield portion of the 9 ms mixing time CLEAN-TOCSY spectrum of HRP^{A1}-CN, and plots of observed *vs* calculated dipolar shifts for protons of heme pocket residues of HRP^{A2}-CN and HRP^{A1}-CN (7 pages). Ordering information is given on any current masthead page.

REFERENCES

Ator, M. A., & Ortiz de Montellano, P. R. (1987) *J. Biol. Chem. 262*, 1542–1551.

Banci, L., Carloni, P., & Savellini, G. G. (1994) *Biochemistry 33*, 12356–12366.

Campbell, I. D., Dobson, C. M., & Ratcliffe, R. G. (1977) *J. Magn. Reson. 27*, 455–463.

Chen, Z., de Ropp, J. S., Hernandez, G., & La Mar, G. N. (1994) *J. Am. Chem. Soc. 116*, 8772–8783.

de Ropp, J. S., La Mar, G. N., Smith, K. M., & Langry, K. C. (1984) *J. Am. Chem. Soc. 106*, 4438–4444.

de Ropp, J. S., Yu, L. P., & La Mar, G. N. (1991) *J. Biomol. NMR 1*, 175–190.

Dunford, H. B. (1991) in *Peroxidases in Chemistry and Biology* (Everse, J., Everse, K. E., & Grisham, M. B., Eds.) Vol. II, pp 1–23, CRC Press; Boca Raton, FL.

Edwards, S. L., & Poulos, T. L. (1990) *J. Biol. Chem. 265*, 2588–2595.

Edwards, S. L., Raag, R., Wariishi, H., Gold, M. H., & Poulos, T. L. (1993) *Proc. Natl. Acad. Sci. U.S.A. 90*, 750–754.

Finzel, B. C., Poulos, T. L., & Kraut, J. (1984) *J. Biol. Chem. 259*, 13027–13036.

Gonzalez-Vergara, E., Meyer, M., & Goff, H. M. (1985) *Biochemistry 24*, 6561–6567.

Hernández, G., Wilks, A., Paolesse, R., Smith, K. M., Ortiz de Montellano, P. R., & La Mar, G. N. (1994) *Biochemistry 33*, 6631–6641.

Hore, P. J. (1983) *J. Magn. Reson. 55*, 283–300.

Kay, E., Shannon, L. M., & Lew, J. Y. (1967) *J. Biol. Chem. 242*, 2470–2473.

La Mar, G. N., & de Ropp, J. S. (1993) in *Biological Magnetic Resonance* (Berliner, L. J., Reuben, J., Eds.) Vol. 12, pp 1–78, Plenum Press, New York.

La Mar, G. N., Hernández, G., & de Ropp, J. S. (1992) *Biochemistry 31*, 9158–9168.

La Mar, G. N., Chen, Z., Vyas, K., & McPherson, A. D. (1995) *J. Am. Chem. Soc. 117*, 411–419.

Morita, Y., Funatsu, J., & Mikami, B. (1993) in *Plant Peroxidases; Biochemistry and Physiology* (Welinder, K. G., Rasmussen, S. K., Penel, C., & Greppin, H., Eds.) pp 1–4, University of Geneva Press, Geneva, Switzerland.

Ortiz de Montellano, P. R. (1987) *Acc. Chem. Res. 20*, 289–294.

Ortiz de Montellano, P. R. (1992) *Annu. Rev. Pharmacol. Toxicol. 32*, 89–107.

Poulos, T. L., & Kraut, J. (1980) *J. Biol. Chem. 255*, 8199–8205.

Reimann, L., & Schonbaum, G. R. (1978) *Methods Enzymol. 52*, 514–521.

Sakurada, J., Takahashi, S., & Hosoya, T. (1986) *J. Biol. Chem. 261*, 9657–9662.

Satterlee, J. D., & Erman, J. E. (1991) *Biochemistry 30*, 4398–4405.

Schonbaum, G. R. (1973) *J. Biol. Chem. 248*, 502–511.

Shannon, L. M., Kay, E., & Lew, J. L. (1966) *J. Biol. Chem. 241*, 2166–2172.

Smith, A. T., Santama, N., Dacey, S., Edwards, M., Bray, R. C., Thornley, R. N. F., & Burke, J. (1990) *J. Biol. Chem. 265*, 13335–13343.

Smith, A. T., Du, P., & Loew, G. H. (1995) in *Nuclear Magnetic Resonance in Paramagnetic Macromolecules* (La Mar, G. N., Ed.) pp 75–93, Kluwer Academic Publishers, Dordrecht, Holland.

Sundaramoorthy, M., Kishi, K., Gold, M. H., & Poulos, T. L. (1994) *J. Biol. Chem. 269*, 32759–32767.

Thanabal, V., de Ropp, J. S., & La Mar, G. N. (1987) *J. Am. Chem. Soc. 109*, 7516–7525.

Thanabal, V., de Ropp, J. S., & La Mar, G. N. (1988) *J. Am. Chem. Soc. 110*, 3027–3035.

Veitch, N. C., & Williams, R. J. P. (1990) *Eur. J. Biochem. 189*, 351–362.

Veitch, N. C., & Williams, R. J. P. (1991) in *Biochemical, Molecular and Physiological Aspects of Plant Peroxidases* (Lobarzewski, J., Greppin, H., Penel, C., & Gaspar, T., Eds.) pp 99–109, University of Geneve Press, Geneva, Switzerland.

Veitch, N. C., Williams, R. J. P., Bray, R. C., Burke, J. F., Sanders, S. A., Thorneley, R. N. F., & Smith, A. T. (1992) *Eur. J. Biochem. 207*, 521–531.

Welinder, K. G. (1992) in *Plant Peroxidase 1980-1990: Topics and Detailed Literature on Molecular, Biochemical, and Physiological Aspects* (Penel, C., Gaspar, T., & Greppin, H., Eds.) pp 1–24, University of Geneva Press, Geneva, Switzerland.

Welinder, K. G., & Gajhede, M. (1993) in *Plant Peroxidases: Biochemistry & Physiology*; (Welinder, K. G., Rasmussen, S. K., Penel, C., & Greppin, H., Eds.) pp 35–42. University of Geneva Press, Geneva, Switzerland.

BI951375D